Feedforward Tracking Controller Design Based on the Identification of Low Frequency Dynamics

E. D. Tung
Graduate Student.

M. Tomizuka
Professor.

Department of Mechanical Engineering,
University of California,
Berkeley, CA 94720

Several methodologies are proposed for identifying the dynamics of a machine tool feed drive system in the low frequency region. An accurate identification is necessary for the design of a feedforward tracking controller, which achieves unity gain and zero phase shift for the overall system in the relevant frequency band. In machine tools and other mechanical systems, the spectrum of the reference trajectory is composed of low frequency signals. Standard least squares fits are shown to heavily penalize high frequency misfit. Linear models described by the output-error (OE) and Autoregressive Moving Average with eXogenous Input (ARMAX) models display better closeness-of-fit properties at low frequency. Based on the identification, a feedforward compensator is designed using the Zero Phase Error Tracking Controller (ZPETC). The feedforward compensator is experimentally shown to achieve near-perfect tracking and contouring of high-speed trajectories on a machining center X-Y bed.

1 Introduction

The objective of tracking control is to follow a desired path as closely as possible. The goal of contouring control is to minimize the perpendicular distance from the actual path to the desired path. Recently, these ideas have become increasingly important in precision manufacturing applications. Such operations as automated arc welding, chip inspection and robot spray painting require mechanical systems to accurately track a desired reference trajectory. One particularly interesting example involves high-speed metal-cutting. A review article on high-speed machining (Coleman, 1992) points out the need for improvement in CNC feed drive servo performance to meet the demands of future high-speed machine tools, where feed rates of 10–30 m/min are required. The goal of this research is the design of effective feedforward control algorithms for high-speed tracking and contouring systems.

Researchers in recent years have investigated the use of digital feedforward controllers to enhance the performance of feedback systems. One such design, the perfect tracking controller (PTC) (Tomizuka, 1987), is used for plants which possess no zeros which are undesirable to cancel (e.g., nonminimum phase zeros or lightly damped oscillatory zeros). The PTC cancels all of the poles and zeros of the feedback system, resulting in an overall transfer function of unity from the desired trajectory to the actual trajectory. For systems with uncancelable zeros, Tomizuka has proposed two feedforward structures. The stable pole zero canceling (SPZC) controller cancels the poles and cancelable zeros of the feedback loop. The zero phase error tracking controller (ZPETC) cancels the closed-loop poles and cancelable zeros and, in addition, eliminates phase error induced by the uncancelable zeros. Xia and Menq (1990) and Haack and Tomizuka (1991) improve upon the ZPETC by adding zeros to the feedforward filter to compensate the system gain error, thereby increasing the bandwidth. Funahashi and Yamada (1992) have analyzed the minimum number of preview steps and the finite settling time nature of ZPETC.

The proposed feedforward controllers assume that a model of the plant (the feedback system) is given. In reality, an accurate discrete-time transfer function for mechanical systems is difficult to obtain, especially when small sampling times are used. Since the Nyquist frequency is inversely proportional to the sampling interval, higher order effects such as amplifier dynamics and notch filters contaminate the identification as the sampling frequency is increased. Kulkarni and Srinivasan (1984) have described the nonlinear effects of amplifier dynamics in machine tool feed drives. Other nonlinearities such as Coulomb friction, stiction and backlash may also corrupt the system identification. For practical implementation, the development of a feedforward tracking controller should consider identification issues.

In this paper, several methodologies are proposed for identifying the dynamics of a system in the frequency band relevant to the design of a feedforward tracking controller. For machine tool feed drives and mechanical systems in general, the power spectrum of typical reference trajectories is composed primarily of low frequency signals. Since the plant to be identified is a closed-loop feedback system with integral control, the performance criterion for each of the methods will be the ability to approximate the system magnitude response at DC, which is unity. As will be shown, the mismatch between the model and the true system is described in the frequency domain by

Contributed by the Dynamic Systems and Control Division for publication in the JOURNAL OF DYNAMIC SYSTEMS, MEASUREMENT, AND CONTROL. Manuscript received by the Dynamic Systems and Control Division July 2, 1992; revised manuscript received January 7, 1993. Associate Technical Editor: A. G. Ulsoy.

a weighting function, which varies between different models depending on the noise description term. Based on the system identification, a digital feedforward compensator is designed to achieve unity gain and zero phase shift over the specified region. The performance of the feedforward controller is then tested on an experimental feed drive system.

The literature contains very few references to practical implementations of feedforward tracking controllers. Suzuki and Tomizuka (1991) describe the implementation of ZPETC on a machine tool servo-system. Tsao and Tomizuka (1987) have developed an adaptive zero phase error tracking controller which identifies the parameters in the feedforward controller in real-time. Kamano et al. (1990) have presented an adaptive feedforward tracking algorithm for positioning systems. Other researchers have explored methods of improving machine tool feed drive performance. Koren (1980) and Kulkarni and Srinivasan (1989) propose several controller structures involving cross-coupling between the axes for improved contouring performance.

The remainder of the paper is organized as follows. In the next section, the equivalence between perfect tracking and the unity transfer function is derived. In Section 3, the experimental test bed is described along with contouring results from an industrial CNC controller. In Section 4, linear least squares identification, analyzed in the frequency domain, is applied to the feed drive system. In Section 5, the system is identified using ARMAX and OE methods.Experimental results are presented in Section 6, and concluding remarks are given in the final section.

2 Perfect Tracking and the Unity Transfer Function

The objective of this research is to design a feedforward tracking controller for a machine tool feed drive system which will perfectly track the desired trajectory $y_d(k)$. This objective is described by the minimization of the penalty function

$$J=\sum_{k=1}^{N}(y_d(k)-y(k))^2 \tag{1}$$

where $y(k)$ is the actual position of the feed drive. The difference equation for the closed-loop plant dynamics relating the reference position $r(k)$ to the actual position $y(k)$ is given by

$$A(z^{-1})y(k)=B(z^{-1})r(k) \tag{2}$$

$$A(z^{-1})=1+a_1z^{-1}+\ldots+a_{na}z^{-na} \tag{3}$$

$$B(z^{-1})=b_1z^{-1}+\ldots+b_{nb}z^{-nb} \tag{4}$$

where $nb \leq na$, and z^{-1} represents a one-step delay. If a feedforward controller is not implemented, the desired position trajectory $y_d(k)$ is used as the reference $r(k)$. Under standard feedback control (e.g., PID), the closed-loop plant cannot perfectly track arbitrary reference trajectories. However, a feedforward controller can compensate for the system dynamics and allows the plant to achieve perfect tracking.

If the system possesses no uncancelable zeros, the feedforward controller is designed by inverting the dynamics of the closed-loop plant (see Fig. 1). The difference equation relating the desired trajectory $y_d(k)$ and the reference $r(k)$ is expressed as

$$A(z^{-1})y_d(k)=B(z^{-1})r(k) \tag{5}$$

By substituting Eq. (5) into Eq. (2) and eliminating $r(k)$, we obtain

$$y(k)+a_1y(k-1)+\ldots+a_ny(k-n)=y_d(k)+a_1y_d(k-1)+\ldots+a_ny_d(k-n) \tag{6}$$

for all k, when $y(k)=y_d(k)$, $-(n-1) \leq k \leq 0$. Hence, by

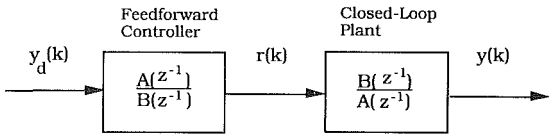

Fig. 1 Feedforward compensator preceding closed-loop plant

using the inverted model of the closed-loop plant as a feedforward compensator, the system can achieve perfect tracking of the desired trajectory.

The design of a feedforward controller relies on an accurate identification of the closed-loop plant. In most mechanical systems, the reference trajectory to be tracked is composed entirely of low frequency signals. For machine tools, the CNC path generator is programmed to limit the maximum acceleration of the desired trajectory, thus constraining the power content of the signal to the low end of the spectrum. For these systems, the identification procedure should focus on the low frequency range. An accurate identification in this region will allow a transfer function of unity gain and zero phase shift to be obtained in the frequency range of the desired trajectory, which will yield perfect tracking. The identification requires the minimization of the following expression

$$J(\theta)=\int_{-\omega_M}^{+\omega_M}|G_0(e^{-j\omega})-G(e^{-j\omega},\theta)|^2d\omega \tag{7}$$

where $G_0(e^{-j\omega})$ is the true system, $G(e^{-j\omega}, \theta)$ is the model of the system, θ represents the parameters in the model, and ω_M represents the highest significant angular frequency component of the reference trajectory. As will be shown in Section 4, this frequency-domain description of the penalty function can be achieved by prefiltering the prediction errors. In practice, this penalty function may produce models with poorly-identified dynamics at high frequency. A more appropriate penalty function which adequately models high frequency dynamics, yet still emphasizes a close fit at low frequency, is given by

$$J(\theta)=\int_{-\pi}^{\pi}|G_0(e^{-j\omega})-G(e^{-j\omega},\theta)|^2Q(\omega,\theta)d\omega \tag{8}$$

where $Q(\omega, \theta)$ has either a flat spectrum or the characteristics of a low-pass filter. A more complete analysis of the frequency-domain description of the penalty function is given in Section 4.

3 Machine Tool Feed Drive System

The experimental test stand for the system identification and feedforward control tests is the X-Y bed of the Matsuura MC510V machining center. The drive train for each axis of the X-Y table consists of an AC motor coupled to a ballscrew which transmits linear displacement of the bed through the ballscrew nut. The MC510V is equipped with a YASNAC Mx-3 CNC controller which provides closed-loop proportional (P) position control for each axis with a sampling period of 2 ms. Several experiments were conducted to measure the frequency response of each axis under both cutting and non-cutting conditions. The results (see Fig. 2) indicate that the bandwidth drops off rapidly for high frequency motion, with no discernible difference between cutting and non-cutting tests. The lack of adequate bandwidth may induce large errors in workpieces machined at high speeds, and makes clear the need for effective feedforward control action.

An experimental feed drive control system was implemented on the machining center, replacing the CNC controller. In its place, motion control was performed on an IBM 80386 PC-AT compatible computer. A block diagram of the experimental control system is shown in Fig. 3. The YASNAC analog servo-pack which performs PI control in the velocity loop was left intact. Position measurements were taken using optical en-

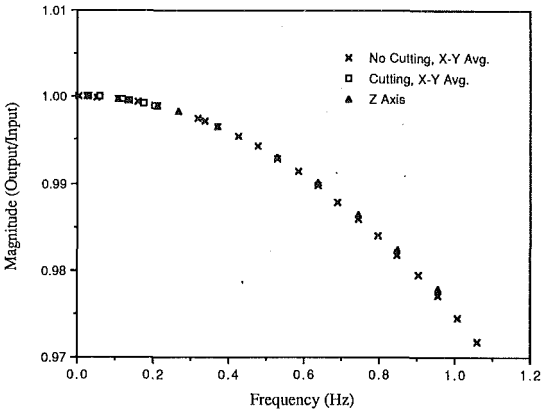

Fig. 2 Magnitude response of the *X*, *Y*, and *Z* axes under cutting and noncutting conditions

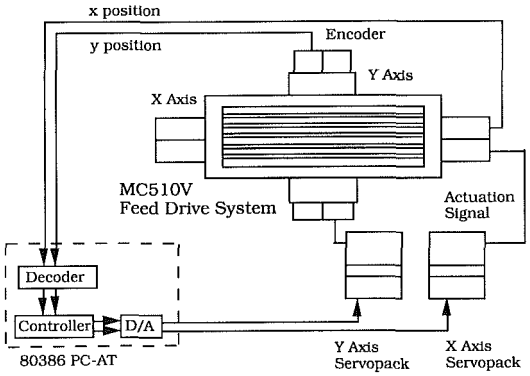

Fig. 3 Experimental feed drive control system

coders on the motor shafts of each axis having a resolution of 1 μm. Special I/O boards residing on the PC-AT performed digital-to-analog conversion of the controller output and decoding of the phase A/phase B encoder signals. The experimental control system used a P control algorithm running at a 2 ms sampling period to emulate the actual system. The plant, either the X or Y axis, is depicted in block diagram form in Fig. 4, where K_p is the proportional control gain in the position loop, K_v and K_i are the proportional and integral control gains in the velocity loop, M_{tot} is the total inertia in the plant, and R_{eq} is the ratio between the linear velocity of the table and the angular velocity of the motor shaft.

4 Least Squares Identification: Frequency Domain Description

This section describes a transformation of the standard least squares penalty function into a frequency domain description. Through a frequency-dependent weighting function, the identification can be biased to emphasize the fit in a particular frequency range. Details of the theoretical development in this section can be found in Ljung (1987).

Consider the penalty function given by the summation of the squared prediction errors

$$J(\theta)=\frac{1}{N}\sum_{k=1}^{N}[y(k)-\phi^T(k,\theta)\theta]^2 \tag{9}$$

where $\phi(k,\theta)$ is the vector of regressors. The penalty function $J(\theta)$ can be shown to be equivalent to the frequency domain penalty function

$$J(\theta)=\frac{1}{2\pi}\int_{-\pi}^{\pi}\Phi_\epsilon(\omega,\theta)d\omega \tag{10}$$

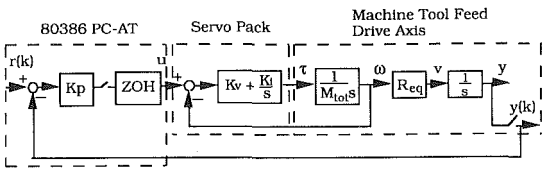

Fig. 4 Closed-loop control system for a single feed drive axis

using an inverse Fourier Transform, where $\Phi_\epsilon(\omega,\theta)$ is the spectrum of the prediction errors.

Now consider the representation of the true system, expressed as

$$y(k)=G_0(z^{-1})u(k)+H_0(z^{-1})e(k) \tag{11}$$

The stochastic noise process described by $v_0(k)=H_0(z^{-1})e(k)$ has the spectrum

$$\Phi_v(\omega)=\lambda_0|H_0(e^{-j\omega})|^2 \tag{12}$$

where $\{e(k)\}$ is a sequence of independent random variables with zero mean values and covariances λ_0. From Theorem 2.2 in Ljung (1987), the spectrum $\Phi_\epsilon(\omega,\theta)$ for the linear model structure given in Eq. (11) is

$$\Phi_\epsilon(\omega,\theta)=\frac{|\tilde{G}(e^{-j\omega},\theta)|^2\Phi_u(\omega)+\Phi_v(\omega)}{|H(e^{-j\omega},\theta)|^2} \tag{13}$$

where $\Phi_u(\omega)$ is the spectrum of the input, $H(e^{-j\omega},\theta)$ is the noise spectrum and $\tilde{G}(e^{-j\omega},\theta)$ is the difference between the spectrum of the actual system and that of the model. After substituting the expression for $\Phi_\epsilon(\omega,\theta)$ into Eq. (10), the frequency domain description of the penalty function becomes

$$J(\theta)=\frac{1}{2\pi}\int_{-\pi}^{\pi}\frac{|G_0(e^{-j\omega})-G(e^{-j\omega},\theta)|^2\Phi_u(\omega)+\Phi_v(\omega)}{|H(e^{-j\omega},\theta)|^2}d\omega \tag{14}$$

Thus, the parameter estimate which minimizes the penalty function can be approximated as

$$\theta^*=\arg\min_{\theta}\int_{-\pi}^{\pi}|G_0(e^{-j\omega})-G(e^{-j\omega},\theta^*)|^2Q(\omega,\theta^*)d\omega \tag{15}$$

The weighting function $Q(\omega,\theta^*)$

$$Q(\omega,\theta^*)=\frac{\Phi_u(\omega)}{|H(e^{-j\omega},\theta^*)|^2} \tag{16}$$

determines the bias distribution in the frequency domain. It may be used to emphasize the fit between the model and the actual system in the frequency region of interest.

The weighting function can be affected through the appropriate selection of the design variables (Wahlberg and Ljung, 1986): the input spectrum $\Phi_u(\omega)$ and the noise model $H(e^{-j\omega},\theta)$. The weighting function can also be adjusted by using a prefilter to filter the prediction errors. Expressing the prediction errors as $\epsilon(k,\theta)$, the filtered prediction errors are described by

$$\epsilon_F(k,\theta)=L(z^{-1})\epsilon(k,\theta) \tag{17}$$

The effect of prefiltering is equivalent to changing the noise model from $H(z^{-1},\theta)$ to

$$H_L(z^{-1},\theta)=[L(z^{-1})]^{-1}H(z^{-1},\theta) \tag{18}$$

The exact effect of changing the design variables in order to affect the bias distribution is not always clear, since the weighting function Q depends on θ^*. Obtaining a satisfactory bias distribution may involve some trial and error. In the following section, examples are given to illustrate the use of the weighting function $Q(\omega,\theta^*)$ in obtaining an accurate identification in the frequency region of interest.

4.1 The ARX Model Structure. Consider the discrete-

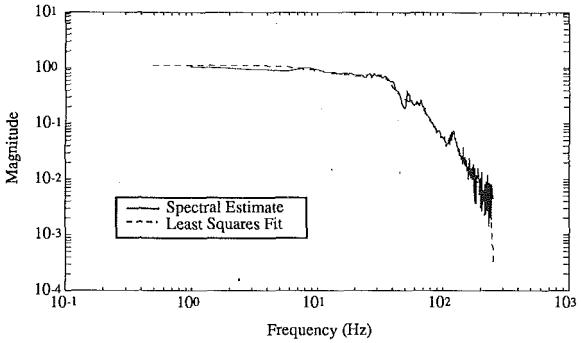

Fig. 5 Least squares fit of Y axis magnitude response using ARX structure: high order model with no prefiltering

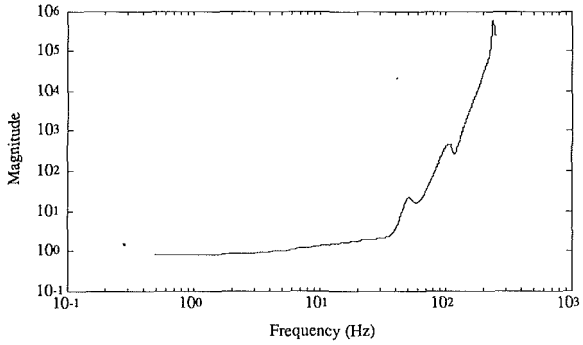

Fig. 6 Magnitude response of $Q(e^{j\omega},\theta)$ using ARX structure: high order model with no prefiltering

time transfer function given by the equation error model structure (ARX structure)

$$A(z^{-1})y(k)=B(z^{-1})u(k)+e(k) \tag{19}$$

where $y(k)$ is the output, $u(k)$ is the input, $e(k)$ is a white noise process and the polynomials $A(z^{-1})$ and $B(z^{-1})$ are given by

$$A(z^{-1})=1+a_1z^{-1}+\ldots+a_{na}z^{-na} \tag{20}$$

$$B(z^{-1})=b_1z^{-1}+\ldots+b_{nb}z^{-nb} \tag{21}$$

The deterministic components of Eq. (19) can be parameterized into the parameter vector and the regression vector as follows

$$\theta=[a_1,\ \ldots,\ a_{na},\ b_1,\ \ldots,\ b_{nb}]^T \tag{22}$$

$$\phi(k)=[-y(k-1),\ \ldots,\ -y(k-na),u(k-1),\ \ldots,\ u(k-nb)]^T \tag{23}$$

The least squares estimate $\hat{\theta}_N$

$$\hat{\theta}_N=\left[\sum_{k=1}^{N}\phi(k)\phi^T(k)\right]^{-1}\sum_{k=1}^{N}[\phi(k)y(k)] \tag{24}$$

minimizes the penalty function given in Eq. (9), where $\phi(k)$ is not a function of θ.

4.1.1 Bias Distribution for ARX Model Structure. The system identification examples described in this section are based on actual input-output data obtained using the experimental feed drive control system. The input consisted of a Gaussian pseudo-random sequence of numbers with a flat spectrum, i.e., $\Phi_u(\omega)=1$ for all ω up to the Nyquist frequency. Each identification was performed using the standard quadratic penalty function described by Eq. (9), with the linear regression predictor given by the ARX structure

$$y(k)=\frac{B(z^{-1})}{A(z^{-1})}u(k)+\frac{1}{A(z^{-1})}e(k) \tag{25}$$

The resulting fits are compared with the transfer function estimates obtained using power spectral methods, in particular, the Welch method (Welch, 1978). The input and output sequences of N points are divided into K sections of M points each (M must be a power of two). Using an M-point FFT, successive sections are windowed using a Hanning window. Fast Fourier transforms are then performed for each section. The spectral estimates are plotted along with the frequency response of the fitted models. While they serve as a useful reference, the main focus in on obtaining good parametric models for feedforward controller design.

Example 1—High Order ARX Model With No Prefiltering. The Y axis of the machining center was modeled using a high order ARX structure, with an order of 16 in the numerator and denominator. The least squares system identification produced the magnitude fit shown in Fig. 5. The fit provides a poor description of the dynamics at low frequency, although the distortion caused by the log scale makes the fit seem reasonable. The magnitude at DC is 1.1360 according to the high order model (should be 1.0). The graph of the frequency weighting function (see Fig. 6) reveals that the fit is heavily biased toward high frequency. The weighting function, given by Eq. (16) in the general case, is equivalent to the squared inverse of the noise model $H(e^{-j\omega},\theta)$ if the input spectrum is flat. Hence, least squares estimation introduces a bias which penalizes high frequency misfit in mechanical systems whose dynamics are typically described by a polynomial $A(e^{-j\omega},\theta)$ which drops off rapidly with increasing frequency. The least squares estimate using the ARX structure was applied for all models up to order 24, resulting in an unsuccessful identification of the low frequency dynamics for each case. Note the presence of notch filters at higher frequencies in the spectral estimate of the plant (see Fig. 5). The high order least squares estimate attempts to accurately model these dynamics while ignoring the low frequency dynamics.

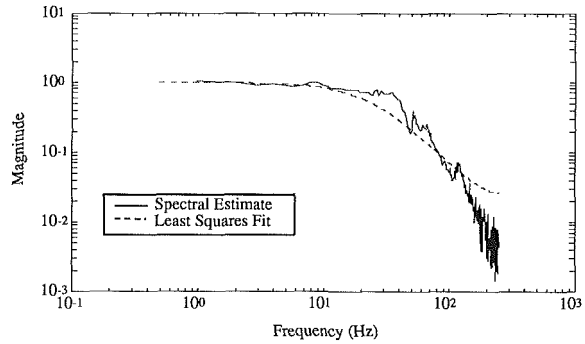

Fig. 7 Least squares fit of Y axis magnitude response using ARX structure: low order model with prefiltering

The notch filters are not present in the X axis servo-pack. The closed-loop dynamics for this axis were modeled using a 10th order system, resulting in an accurate fit at low frequency (identified DC gain is 1.0047).

Example 2—Low Order ARX Model With Prefiltering. A low order model given by

$$y(k)=\frac{b_1z^{-1}}{1+a_1z^{-1}+a_2z^{-2}}u(k)+\frac{1}{1+a_1z^{-1}+a_2z^{-2}}e(k) \tag{26}$$

was used in identifying the Y axis system. As opposed to the previous example, a prefilter was used to manipulate the frequency weighting function. The resulting magnitude plot is shown in Fig. 7. The model yields a reasonable description of the system dynamics in the low frequency region. The prefilter, a third order Butterworth low-pass filter with a cutoff frequency of 10 Hz, serves to counteract the high-pass characteristics of the unfiltered $Q(\omega,\theta^*)$

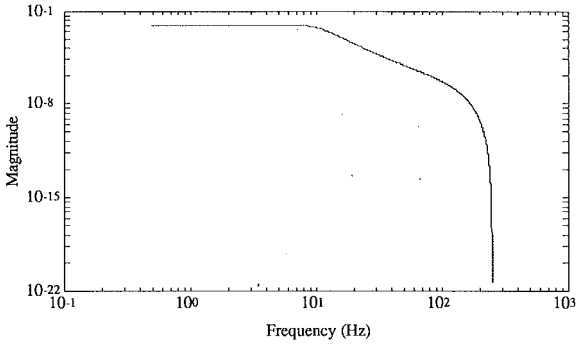

Fig. 8 Magnitude response of $Q(e^{j\omega},\theta)$ using ARX structure: low order model with prefiltering

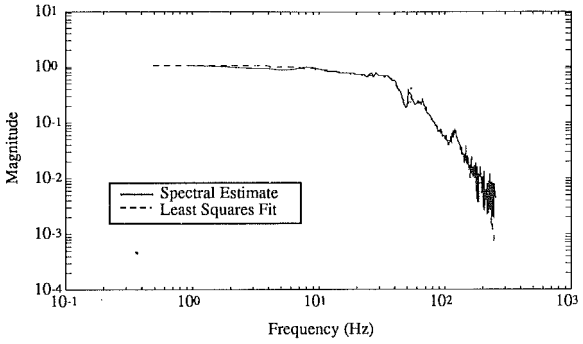

Fig. 9 Least squares fit of Y axis magnitude response using ARMAX structure

$$Q(\omega,\theta^*)=\frac{\Phi_u(\omega)L(e^{-j\omega})}{|H(e^{-j\omega},\theta^*)|^2} \tag{27}$$

The magnitude plot of the weighting function (see Fig. 8) clearly reflects the emphasis on a low-frequency fit. The magnitude at DC predicted by the least squares estimate is 0.9745. Although the weighting function is strong at low frequency, the model does not have enough degrees of freedom to accurately describe the dynamics.

4.1.2 Summary of Least Squares Identification. High order ARX models are necessary to accurately describe the dynamics of a machine tool feed drive over the entire spectrum. In the example where higher order effects, such as notch filters, are pronounced, the ARX model is inadequate because of its limited ability to describe the noise term. In either case, the high order estimates are less than ideal for the design of a feedforward tracking controller. The high frequency bias is partially compensated by the use of prefilters. The problem with prefiltering is that by removing the high frequency dynamics, the filtered system is strongly susceptible to being "overworked," i.e., the system becomes overmodeled. An overworked system has an inverse term in the least squares solution (see Eq. (24)) which is rank deficient. For the feed drive system, no meaningful estimates could be generated for models with orders higher than 3 with a fit biased toward low frequency. The $A(e^{-j\omega},\theta)$ polynomial of the estimate drops off so rapidly that it is practically impossible to find an appropriate low pass filter which can compensate for the bias without forcing the least squares estimate to become singular.

4.2 Constrained Least Squares. The plant to which the identification techniques are applied is a closed-loop feedback system with integral control. From control theory, the magnitude of the transfer function for such a system at DC is unity. This fact can be used in a constrained least squares estimation. The coefficients of the polynomials $A(z^{-1})$ and $B(z^{-1})$ must obey the constraint

$$1+a_1+a_2+\ldots+a_{na}=b_1+b_2+\ldots+b_{nb} \tag{28}$$

By rearranging the terms and by using the parameter vector of Eq. (22), the above equation can be expressed as

$$r\theta=s \tag{29}$$

where s is a scalar and r has the dimensions of the transpose of θ. This constraint is adjoined to the quadratic penalty function given by Eq.(9), resulting in a new penalty function

$$J(\theta)=\sum_{k=1}^{N}[y(k)-\phi^T(k)\theta]^2+\lambda(r\theta-s) \tag{30}$$

The solution to the constrained least squares problem is obtained by taking derivatives of the penalty function with respect to θ and the Lagrange multiplier λ and setting the resulting expressions equal to zero (Stang,1986). An analytic expression for θ and λ is given by the following equation

$$\begin{bmatrix}\theta\\ \lambda\end{bmatrix}=\begin{bmatrix}2\sum_{k=1}^{N}\phi(k)\phi^T(k) & r^T\\ r & 0\end{bmatrix}^{-1}\begin{bmatrix}2\sum_{k=1}^{N}\phi(k)y(k)\\ s\end{bmatrix} \tag{31}$$

This method was applied in conjunction with the frequency-weighting techniques in the identification of the dynamics of the closed-loop plant at low frequencies.

5 Other Model Structures

The ARX model structure has the property that the predictor defines a linear regression. While other model structures may offer more flexibility in describing the error term, they are more difficult to apply because the predictor does not describe a linear regression. One common example is the ARMAX model given by

$$A(z^{-1})y(k)=B(z^{-1})u(k)+C(z^{-1})e(k) \tag{32}$$

The predictor for this model is expressed as

$$\hat{y}(k)=\phi^T(k,\theta)\theta \tag{33}$$

where the regression vector $\phi^T(k,\theta)$ is a function of the parameters (Ljung, 1987). The solution to the least squares minimization for these *pseudolinear regressions* involves complicated iterative techniques.

One other notable model is the output error (OE) structure

$$y(k)=\frac{B(z^{-1})}{F(z^{-1})}u(k)+e(k) \tag{34}$$

The coefficients of $F(z^{-1})$ are $f(=(1, f_1, \ldots, f_{nf})$ and the coefficients of $B(z^{-1})$ are $b=(b_1, \ldots, b_{nb})$. Notice that the noise model $H(z^{-1},\theta)=1$, so that if no prefiltering is used, the frequency-weighting function $Q(\omega,\theta^*)=1$ for all ω.

5.1 ARMAX Identification. A model described by the ARMAX structure given in Eq. (32) was applied to the Y axis input-output data. The ARMAX estimate is generated by an iterative Gauss-Newton algorithm (Matlab, 1987). The magnitude response of the estimate (eighth order) is given in Fig. 9. The DC gain is predicted to be 1.0110, a good approximation. The magnitude of the frequency weighting function, shown in Fig. 10, reveals that high frequency misfit is more heavily penalized. Since the weighting function is expressed as the square of the inverse of the noise model, the ARMAX structure introduces a bias toward high frequency, although not nearly as strong a bias as for the ARX structure. The plots of the autocorrelation function for the residuals and the cross-correlation between the input and the residuals are given in Figs. 11 and 12. Since both fall within the 95 percent confidence limits, the identified model is valid. Similar results were obtained for a sixth order model of the X axis.

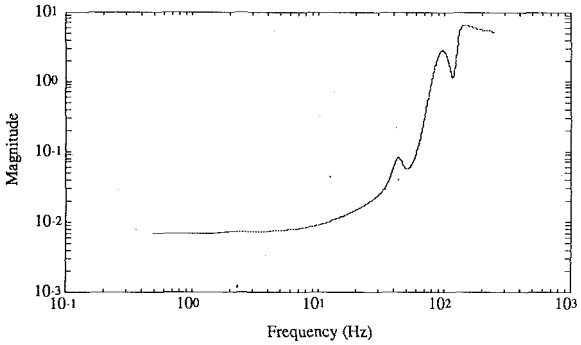

Fig. 10 Magnitude response of $Q(e^{j\omega},\theta)$ using ARMAX structure

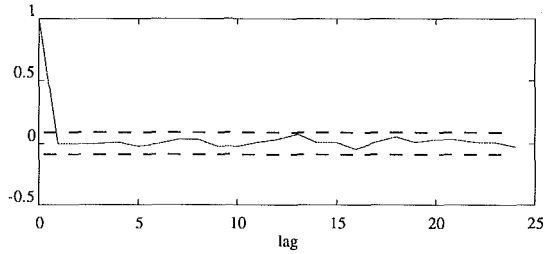

Fig. 11 Autocorrelation function of residuals for Y axis fit using ARMAX structure

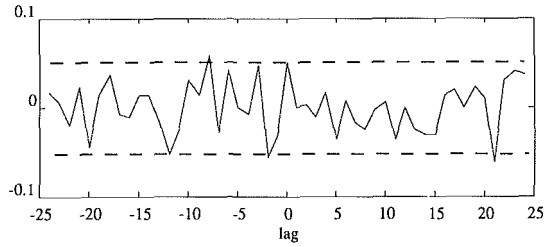

Fig. 12 Cross-correlation function between input and residuals for Y axis fit using ARMAX structure

5.2 Output Error Identification. A model described by the output error (OE) structure given in Eq. (34) was estimated using an iterative Gauss-Newton algorithm. For the X axis, a fifth order model was obtained with coefficients $b=(0, 0.0051, 0.0549, -0.0193, -0.0135)$ and $f=(1, -2.7674, 3.297, -2.0807, 0.6626, -0.0844)$. The magnitude and phase responses of the system are given in Figs. 13 and 14. The gain at DC is estimated to be 1.0060, an extremely good prediction. Since no prefiltering is applied, the frequency weighting function is unity. The best validation criterion for the OE model is the cross-correlation function (see Fig. 15), which shows that the model is valid. The OE model is not concerned with producing a white error spectrum, so the autocorrelation function is not revelant. One drawback of the OE model is that the computational algorithm sometimes converges to a local minimum. The result is dependent on the initial values (Ljung, 1987).

The Y axis dynamics are similarly modeled, with good results obtained using a 7th order model. The DC gain is estimated as 1.0065.

5.3 Summary of OE and ARMAX Structures. The output error and ARMAX model structures both provided accurate identification of the dynamics near DC while requiring relatively low order models. The output error structure demonstrated slightly better results, as predicted through the plots of the weighting function. Both models provide accurate identification of the dynamics in the desired range while keeping the model order low. The identification results for the ARX, OE, and ARMAX structures are summarized in Table 1.

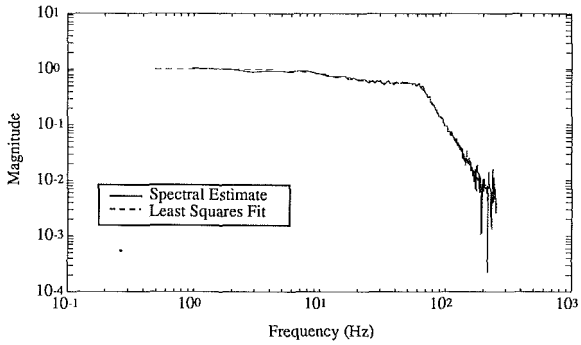

Fig. 13 Least squares fit of X axis magnitude response using OE structure

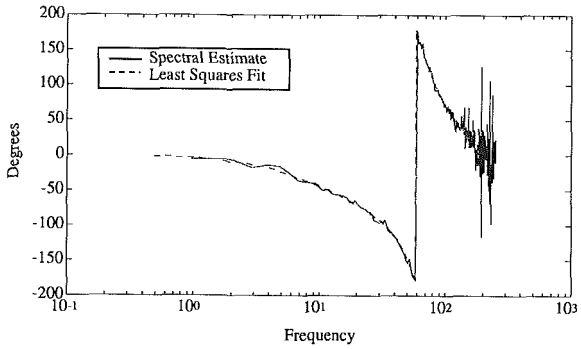

Fig. 14 Least squares fit of X axis phase response using OE structure

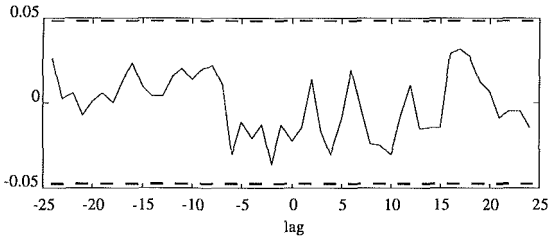

Fig. 15 Cross-correlation between input and residuals for X axis fit using OE structure

Table 1 Identification results: model order and DC gain for ARX, OE, and ARMAX structures

Model Structure	X Axis (no notch filters)		Y Axis (notch filters)	
	Order	DC Gain	Order	DC Gain
ARX	10th	1.0047	16th	1.1360
ARX w/prefiltering	2nd	0.9745	2nd	1.0249
ARMAX	6th	1.0104	8th	1.0110
OE	5th	1.0060	7th	1.0065
OE w/prefiltering	5th	1.0048	5th	1.0132

5.4 Constrained Minimization. A constrained minimization can be performed for the OE and ARMAX models using the constraint equation given by Eq. (28). As described previously, the prediction error for these models describes a pseudolinear regression which requires an iterative search for the minimum.

6 Feedforward Tracking Control

In the previous section, a methodology was presented to precisely identify the dynamics of a system in the desired frequency range, resulting in a discrete-time transfer function estimate. The identified model is now used to design a feedforward compensator. The identification procedures in Sections 4 and 5 consistently produced models with zeros outside

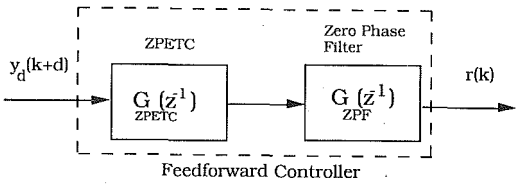

Fig. 16 Feedforward tracking controller design using zero phase filtering

the unit circle. Astrom and Wittenmark (1984) have noted that unstable zeros are very common in digital control, especially when the sampling time is small.

Several feedforward schemes have been proposed for nonminimum phase systems. The zero phase error tracking controller (Tomizuka, 1987) cancels the closed-loop poles and cancelable zeros and eliminates the phase error induced by the uncancelable zeros. Consider the asymptotically stable closed-loop plant described by

$$G(z^{-1}) = \frac{y(k)}{r(k)} = \frac{z^{-d}B(z^{-1})}{A(z^{-1})} = \frac{z^{-d}B^{-}(z^{-1})B^{+}(z^{-1})}{A(z^{-1})} \tag{35}$$

where d is the number of delay steps, $B^{+}(z^{-1})$ represents the cancelable portion of $B(z^{-1})$ and $B^{-}(z^{-1})$ represents the uncancelable portion. The ZPETC is given by

$$G_{ff}(z^{-1}) = \frac{r(k)}{y_d(k)} = \frac{z^{d}A(z^{-1})B^{-}(z)}{B^{+}(z^{-1})[B^{-}(1)]^2} \tag{36}$$

where $B^{-}(z)$ is obtained by replacing z^{-1} in $B^{-}(z^{-1})$ by z. Xia and Menq (1990) and Haack and Tomizuka (1991) propose adding zeros to the ZPETC to reduce the gain error. In this paper, the standard ZPETC is used in the design of the feedforward compensator.

One special property of servo systems in machining is that the desired trajectory, generated by the CNC interpolator, is known in advance. Hence, the feedforward controller can use step-ahead information in canceling the effect of delays in the servo loop. Typical CNC reference generators create trajectories with linear or exponential acceleration/deceleration profiles which contain no significant power spectral content above 1 Hz.

The feedforward compensator amplifies the power spectrum of the reference trajectory at higher frequencies to compensate for low bandwidth in the closed-loop plant. In doing so, it may introduce oscillations into the modified reference trajectory $r(k)$. To avoid exciting these resonances and to ensure a smooth trajectory, the feedforward compensator should also include a low pass filter. A causal filter is not recommended because it distorts the zero phase shift properties in the decade preceding the cutoff frequency. A good choice is a zero phase filter (ZPF),

$$G_{ZPF}(z,z^{-1}) = \frac{\alpha_m z^m + \alpha_{m-1}z^{m-1} + \ldots + \alpha_1 z + \alpha_0 + \alpha_1 z^{-1} + \ldots + \alpha_m z^{-m}}{2\alpha_m + 2\alpha_{m-1} + \ldots + \alpha_0} \tag{37}$$

a moving average FIR filter with low pass characteristics and zero phase shift over all frequency. Since future information is available, the acausality of the ZPF does not hinder its use. The ZPF is combined with the ZPETC to form the complete design of the feedforward controller (see Fig. 16).

6.1 Experimental Results. The feedforward controller for the X axis was designed using ZPETC, a ZPF with $m = 3$, and a 5th order model from the OE identification described in Section 5.2. For the Y axis, a 5th order model from an OE identification was used in the design.

The overall system transfer function for each axis was derived by passing a white noise signal with a flat spectrum

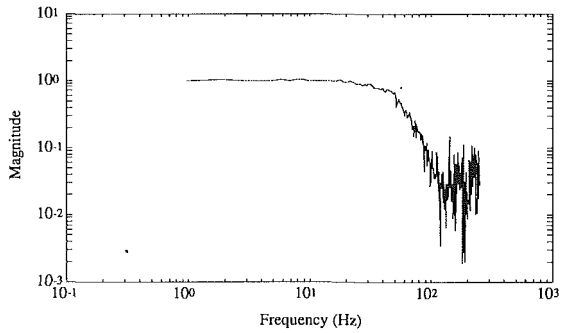

Fig. 17 X axis experimental magnitude response under feedforward tracking control

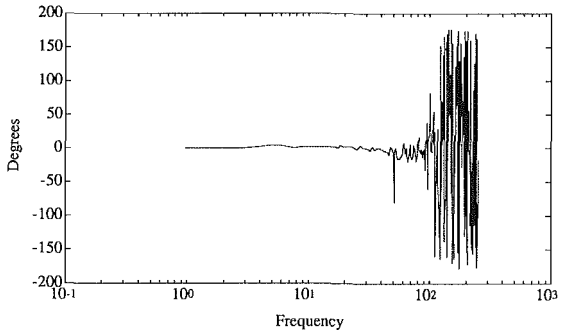

Fig. 18 X axis experimental phase response under feedforward tracking control

through the feedforward compensator and the plant. The magnitude and phase responses for the X axis are depicted in Figs. 17 and 18. Notice that the magnitude is approximately unity and the phase is close to zero in the low frequency region up to 20 Hz. This implies perfect tracking of reference trajectories whose power spectral content is contained in this region. The feedforward controller was used to enhance the tracking performance for a trajectory with a trapezoidal velocity profile (maximum speed 3000 mm/min) and a 0.6 Hz sinusoid. As shown in Figs. 19 and 20, the feedforward compensator achieves near-perfect tracking, and clearly demonstrates superior performance over the uncompensated system. The tracking errors for the trapezoidal velocity profile using the feedforward controller are shown in Fig. 21. The two large spikes in the error signal are caused by low velocity friction. The maximum tracking error over the remainder of the trajectory (over 1000 points) is less than 6 microns. Tung et al. (1993) have proposed a method using planned feedforward inputs to overcome the friction effects.

For two-axis tracking, an appropriate measure of the accuracy of the controller is the contouring error, the perpendicular distance from the desired path to the actual path (Koren, 1980). The contouring performance of the X and Y axis feedforward controllers was tested for a high frequency (2 Hz) 10 mm radius circle. The contouring errors for the compensated and uncompensated systems are graphed in Fig. 22. Despite the deleterious effects of low velocity friction, the feedforward compensator is able to achieve a near-perfect contour of the desired circle. It should be noted that the proportional gain in the experimental controller was tuned for high performance tracking. In the actual CNC controller, the proportional gain is set quite small to avoid exciting resonances in the machine tool. The RMS contouring error for the CNC controller is estimated to be 900 μm (extrapolated from Fig. 2), as opposed to 2.8 μm and 106.8 μm for the experimental controller with and without feedforward compensation, respectively. In Fig. 23, the contouring errors for a 0.6 Hz circle of radius 13 mm is displayed. Using feedforward friction compensation with

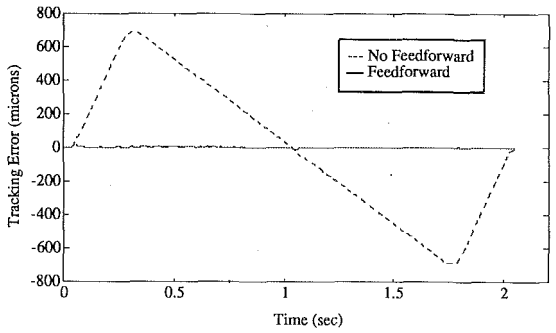

Fig. 19 *X* axis experimental tracking performance for trajectory with trapezoidal velocity profile

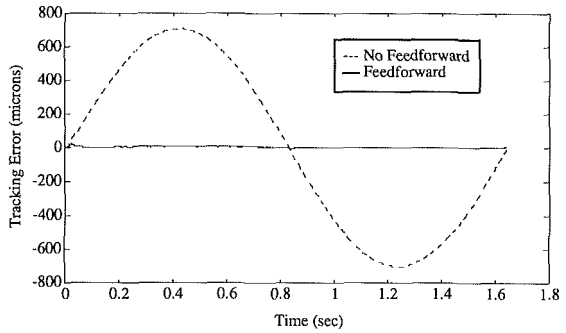

Fig. 20 *Y* axis experimental tracking performance for 0.6 Hz sinusoid

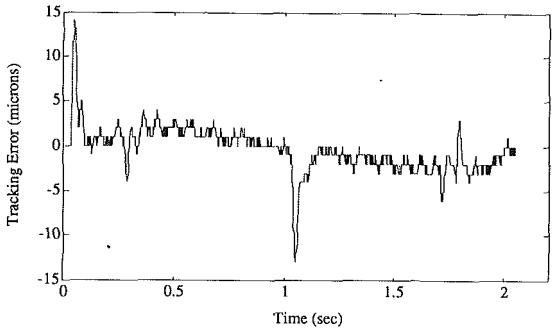

Fig. 21 *X* axis experimental tracking performance using the zero phase error tracking controller

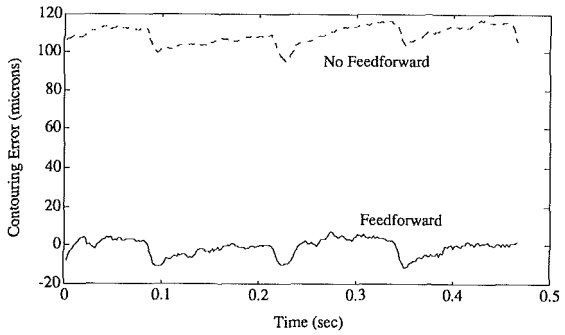

Fig. 22 Experimental contouring performance for high frequency (2 Hz) circular trajectory

the ZPETC, the maximum contouring error is under 4 microns over the entire circle.

Feedforward tracking experiments were also conducted using low order models of the ARX structure with prefiltering of the prediction errors (Tung and Tomizuka, 1992). While the identification methodology and feedforward controller design procedure are more rigorously treated in this paper, the experimental results are similar.

7 Conclusions

Several methodologies for identifying the dynamics of machine tool feed drive systems have been presented. By accurately identifying the dynamics in the desired frequency region, an effective feedforward tracking controller can be designed. Servo-system identification is a difficult problem, especially when small sampling times are used. Previous research in feedforward tracking control has not emphasized identification.

The simplest method is the linear least squares estimate, which has been shown to penalize high frequency misfit in mechanical systems. A high order model is often required to accurately model low frequency dynamics. In some cases, the estimate will not converge to a satisfactory result in this region. The biasing problem can be somewhat alleviated by prefiltering the prediction errors. However, this can lead to "overworking" the model as the order is increased. An iterative scheme has been used to estimate parameters in the OE and ARMAX structures. The OE model does not contain a noise description term, and has a flat weighting spectrum if a white-noise input is used. Accurate descriptions of the dynamics at low frequency may be obtained using this structure, while maintaining a modest order. Similarly, good models may be determined through the ARMAX structure. It is recommended that these models be used in the design of feedforward tracking controllers. The identified plant is a closed-loop feedback system using integral control with a gain of unity at DC. This fact was used to perform a constrained least squares minimization for each model structure.

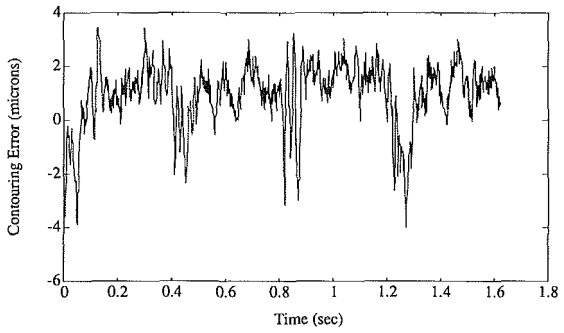

Fig. 23 Experimental contouring performance using feedforward control with friction compensation, 0.6 Hz, 13 mm radius circle

Using the identified model of the closed-loop system, a feedforward controller for the machine tool feed drive system was designed based on the ZPETC. The feedforward compensator demonstrated near-perfect tracking of high-speed reference trajectories. Nonlinear effects such as friction tended to slightly degrade performance. Contouring performance was significantly improved.

References

Astrom, K., and Wittenmark, B., 1984, *Computer Controlled Systems*, Prentice-Hall, Englewood Cliffs, NJ.

Coleman, J. R., 1992, "No-Myth High-Speed Machining," *Manufacturing Engineering*, Oct., pp. 61–65.

Funahashi, Y., and Yamada, M., 1992, "Generalization of Zero Phase Error Tracking Controller," *Transactions of the Society of Instrument and Control Engineers*, Vol. 28, No. 1, pp. 59–66 (in Japanese).

Haack, B., and Tomizuka, M., 1991, "The Effect of Adding Zeroes to Feedforward Controllers," ASME JOURNAL OF DYNAMIC SYSTEMS, MEASUREMENT, AND CONTROL, Vol. 113, No. 1, pp. 6–10.

Kamano, T., Suzuki, T., Kuzuhara, T., and Tomizuka, M., 1990, "Feedback Plus Adaptive Feedforward Control for Positioning System with Progressive Wave Type Ultrasonic Motor," *Proceedings of the 1990 Japan-USA Symposium on Flexible Automation*, Kyoto, Japan, pp. 601–607.

Koren, Y., 1980, "Cross-Coupled Biaxial Computer Controls for Manufacturing Systems," ASME JOURNAL OF DYNAMIC SYSTEMS, MEASUREMENT, AND CONTROL, Vol. 102, No. 1, pp. 265–272.

Kulkarni, P. K., and Srinivasan, K., 1984, "Identification of Discrete Time Dynamic Models for Machine Tool Feed Drives," *Proceedings of the Symposium on Sensors and Controls for Automated Manufacturing and Robotics*, ASME Winter Annual Meeting, New Orleans, LA, pp. 1–12.

Kulkarni, P. K., and Srinivasan, K., 1989, "Optimal Contouring Control of Multi-Axial Feed Drive Servomechanisms," ASME *Journal of Engineering for Industry*, Vol. 111, No. 2, pp. 140–149.

Ljung, L., 1987, *System Identification: Theory for the User*, Prentice-Hall, Inc., Englewood Cliffs, NJ.

Matlab User's Manual, The MathWorks, Inc., 1987.

Strang, G., 1986, *Introduction to Applied Mathematics*, Wellesley-Cambridge Press, Wellesley, MA.

Suzuki, A., and Tomizuka, M., 1988, "Design and Implementation of Digital Servo Controller for High Speed Machine Tools," *Proceedings of the 1991 American Control Conference*, Vol. 2, Boston, MA, pp. 1246–1251.

Tomizuka, M., 1987, "Zero Phase Error Tracking Algorithm for Digital Control," ASME JOURNAL OF DYNAMIC SYSTEMS, MEASUREMENT, AND CONTROL, Vol.109, No. 1, pp. 65–68.

Tsao, T. C., and Tomizuka, M., 1987, "Adaptive Zero Phase Error Tracking Algorithm for Digital Control," ASME JOURNAL OF DYNAMIC SYSTEMS, MEASUREMENT, AND CONTROL, Vol.109, No. 4, pp. 349–354.

Tung, E. D., Anwar, G., and Tomizuka, M., 1993, "Low Velocity Friction Compensation and Feedforward Solution Based on Repetitive Control," ASME JOURNAL OF DYNAMIC SYSTEMS, MEASUREMENT, AND CONTROL, Vol. 115, No. 2A, pp. 279–284.

Tung, E. D., and Tomizuka, M., 1992, "Application of Frequency-Weighted Least Squares System Identification to Feedforward Tracking Controller Design," *Proceedings of the 1992 Japan-USA Symposium on Flexible Automation*, Vol. 1, San Francisco, CA, p. 503–510.

Wahlberg, B., and Ljung, L., 1986, "Design Variables for Bias Distribution in Transfer Function Estimation," *IEEE Transactions on Automatic Control*, Vol. AC-31, pp. 134–144.

Welch, P. D., 1978, "The Use of Fast Fourier Transform for the Estimation of Power Spectra: A Method Based on Time Averaging over Short, Modified Periodograms," *Modern Spectrum Analysis*, D. G. Childers, ed., New York, Wiley, pp. 17–20.

Xia, Z., and Menq, C-H., 1990, "Precision Tracking Control of Nonminimum-Phase Systems and its Application to Noncircular Cutting," *Automation of Manufacturing Processes*, K. Danai and S. Malkin, eds., DSC-Vol. 22, pp. 95–99.